https://doi.org/10.15407/ujpe68.2.132

YU.F. ZABASHTA, V.I. KOVALCHUK, O.S. SVECHNIKOVA, S.V. KONDRATENKO,
S.O. ALEKSEEV, A.V. BRYTAN, L.YU. VERGUN, L.A. BULAVIN

Taras Shevchenko National University of Kyiv, Faculty of Physics
(64/13, Volodymyrs'ka Str., Kyiv 01601, Ukraine)

FEATURES OF THE FORMATION OF A NETWORK IN SOLUTIONS OF RIGID-CHAIN POLYMERS

It has been shown that the network in rigid-chain polymer gels has a specific shape: the role of nodes in this network is played by flat aggregates formed by folded polymer chains. A mechanism for the emergence of such a network has been proposed, and its existence in metolose hydrogels has been confirmed experimentally using the dynamic light scattering and atomic force microscopy methods.

Keywords: polymer network, dynamic light scattering, atomic force microscopy.

1. Introduction

When characterizing the polymer chains, the following spatial scales are introduced [1]: the vector $\mathbf{R}$ connecting the chain ends, the chain link size a, the size of chain segment (the rigid section of the chain) ℓ, and the length L of the chain in the stretched state. There are the following relationships between those quantities:

$$L = Na, \tag{1}$$

$$\langle \mathbf{R}^2 \rangle = L\ell, \tag{2}$$

where N is the number of links in the chain, and $\langle \mathbf{R}^2 \rangle$ is the average value of $\mathbf{R}^2$.

There are two classes of polymers: flexible-chains, for which the condition

$$\ell \gtrsim a \tag{3}$$

is fulfilled, and rigid-chains, which are characterized by the inequalities

$$a \ll \ell \ll L. \tag{4}$$

It is also known [2] that there can exist two types of structures in a polymer solution: the sol and gel structures. In contrast to the sol structure case, the polymer chains in the gel structure form a network. Under certain conditions, a sol-gel transition takes place at which the sol structure transforms into the gel one. The gel formed in an aqueous polymer solution is called the hydrogel.

The generally accepted model of the network in the polymer is a model [3–5] in which the network nodes are connected via polymer chains (Fig. 1). A characteristic feature of this model is the hierarchy of spatial scales,

$$\ell_1 \ll \ell_2, \tag{5}$$

where ℓ_1 is the node size, and ℓ_2 is the average distance between the nodes. For condition (5) to be sat-

---

Citation: Zabashta Yu.F., Kovalchuk V.I., Svechnikova O.S., Kondratenko S.V., Alekseev S.O., Brytan A.V., Vergun L.Yu., Bulavin L.A. Features of network formation in solutions of rigid-chain polymers. *Ukr. J. Phys.* **68**, No. 2, 132 (2023). https://doi.org/10.15407/ujpe68.2.132.

Цитування: Забашта Ю.Ф., Ковальчук В.І., Свечнікова О.С., Кондратенко С.В., Алексєєв С.О., Британ А.В., Вергун Л.Ю., Булавін Л.А. Особливості утворення сітки в гелях жорстколанцюгових полімерів. *Укр. фіз. журн.* **68**, №2, 132 (2023).

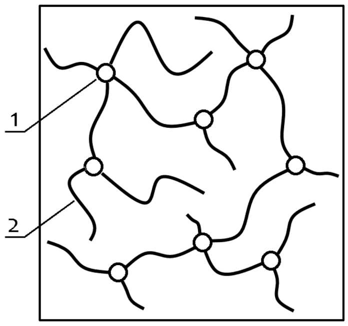

Fig. 1. A model of a polymer network formed by flexible chains: node (*1*), chain (*2*)

isfied, the node size must be much smaller than the chain length L. Such a node can only be formed by flexible chains, and, therefore, the model shown in Fig. 1 is acceptable only for flexible-chain polymers.

So, what does the network in rigid-chain polymers look like, and what is the mechanism of its formation? To answer these questions, we studied the aqueous solutions of rigid-chain polymers [6–13]. As the research object, typical representatives of the polymers belonging to this class, cellulose derivatives, were chosen. This choice was also done because of the needs of modern medicine, where the gels of mentioned polymers are used; in particular, these are ophthalmology [14, 15], tissue engineering [16, 17], drug delivery systems [18, 19], and the treatment of wounds [20–23].

In works [6, 7, 11, 12], the preconditions for a polymer network to be formed in the aqueous solutions of cellulose derivatives were studied. In this paper, we propose a mechanism of network formation in the indicated hydrogels.

2. Experimental Part

The aqueous solution (1.5 g/l) of metolose 65SH-50 produced by Shin-Etsu Chemical Co. (Tokyo, Japan) was studied [24]. The molecular weight of this compound $M = 88000$ [25], and the substitution type is 2906 [26].

Dynamic light scattering in the researched solution was studied making use of a Zetasizer Nano ZS (Malvern) device. The experimental results are shown in Fig. 2, where the dependence of the average size of the clusters available in the solution on the solution temperature T is depicted. As one can see, the cluster sizes at $T > 65$ °C significantly exceed the corresponding values at $T < 65$ °C.

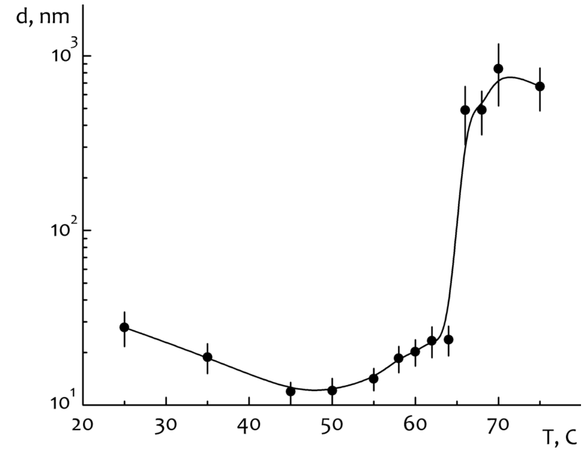

Fig. 2. Dependence of the average cluster size d on the temperature T

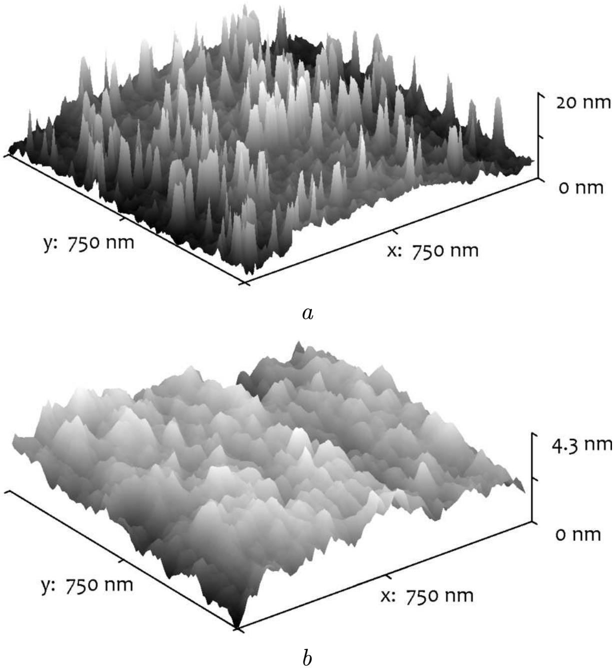

Fig. 3. Reliefs of the film surface obtained at the temperatures $T = 50$ °C (*a*) and 70 °C (*b*)

An atomic force microscope Integra Prima Basic (NT-MDT Spectrum Instruments) and the Gwyddion software [27] were applied to study the surface structure of the films obtained as a result of the metolose solution epitaxy on a glass substrate at the temperatures $T = 50$ °C and 70 °C. The experimental results are exhibited in Fig. 3. As is seen, the roughness of the surface obtained at $T = 50$ °C substantially exceeds that at the surface obtained $T = 70$ °C.

3. Discussion of Experimental Results

Let us determine the shape that a polymer cluster has at $T = 50$ °C. In work [7], on the basis of viscometric experiments, it was found that, at this temperature, metolose clusters have the form of elongated ellipsoids of rotation, for which the ratio between the lengths of the axes equals

$$H/D \cong 70. \tag{6}$$

Denoting the molecular weight of a polymer link as m, let us write

$$N = M/m. \tag{7}$$

According to work [28], we have $m = 162$ and $a = 1$ nm for a cellulose chain. Substituting these values into formulas (1) and (7), we get $N = 530$ and $L = 530$ nm.

A large value of the ratio H/D allows the indicated ellipsoid to be approximately considered as an $H \times D \times D$-parallelepiped, where H and D are the lengths of its sides. To describe the chain behavior, the persistent model [1] will be used, in which the chain is considered as a uniform cylinder with diameter d_1. Based on the crystalline structure of cellulose [28], we put $d_1 = 0.8$ nm.

In order to form an $H \times D \times D$-parallelepiped from the chain, it is necessary to divide the chain, not breaking it, into sections each with length H and arrange them in parallel to each other. Then, the number of such sections equals

$$n = L/H. \tag{8}$$

Evidently, the indicated procedure must also satisfy the equality

$$n\pi {d_1}^2/4 = D^2. \tag{9}$$

Now, by solving the system of equations (6), (8), and (9), we obtain $n \approx 5$, $D \approx 1.5$ nm, and $H \approx 105$ nm. These values were calculated according to the data of the viscometric experiment [7]. Let us demonstrate that they agree with the value $d_{\mathrm{DLS}} = 12.1$ nm obtained for the average size of polymer clusters at $T = 50$ °C using the method of dynamic light scattering (see Fig. 2).

It is known [29] that the information about the size of clusters can be obtained from the data on dynamic light scattering using the theory [30] describing the diffusion of spherical particles. The mobility of such particles is determined by the formula

$$u = (3\pi\eta\, d_{\mathrm{DLS}})^{-1}, \tag{10}$$

where η is the viscosity of the liquid in which the particles move. As follows from the determination formula for u, the diffusing particle is characterized by only one size, d_{DLS}. In our case where the particle is an ellipsoid of rotation, we can obtain the quantity d_2 possessing the length dimensionality as follows:

$$d_2 = \sqrt{HD}. \tag{11}$$

Substituting the above H- and D-values into formula (11), we obtain $d_2 = 12.6$ nm, which practically coincides with the d_{DLS}-value and makes it possible to talk about the consistency of the results obtained for the cluster size using the viscometric method and the method of dynamic light scattering.

Note that the values for d_2 that are close to d_{DLS} can also be calculated

(i) from Perrin's formula [31, 32] for the diffusion of ellipsoids,

$$d_2 = 2/S, \quad S = \int\limits_0^\infty \frac{dx}{(D^2 + x)\sqrt{(H^2 + x)}}, \tag{12}$$

which gives $d_2 = 10.3$ nm; and

(ii) from the formula for the diffusion of rigid rods [33],

$$d_2 = \frac{H}{2\ln(2H/D)}, \quad H \gg D, \tag{13}$$

which gives $d_2 = 10.6$ nm.

In work [12], it was experimentally established that the formation of a polymer network from rigid chains results in an additional reflection of incident light. The intensity of reflected light increases, as the volume occupied by the formed network grows. After the sol-gel transition is completed, practically all incident light is reflected by the gel structure.

In the framework of the network model shown in Fig. 1, it is impossible to explain the additional light reflection observed in work [12]. However, this phenomenon can be described using a network model that contains elements able to effectively reflect light. In particular, such elements can be flat aggregates of polymer chains. If such aggregates are available, the network looks like that shown in Fig. 4. In essence, these aggregates play the role of nodes.

In our opinion, the anomaly observed in the behavior of the dependences $d_{\rm DLS}(T)$ at $T = 70$ °C (see Fig. 2) has the same nature as the light reflection effect detected in work [12]. Namely, it testifies to the appearance of large flat aggregates formed by polymer chains. Let us assume that the possible mechanism giving rise to the emergence of such aggregates consists of two stages.

At the first stage, the globules unfold. More specifically, the globules are transformed from ellipsoids (in the accepted approximation, they are parallelepipeds) into sheets, each formed by five fold chains (Fig. 5). The thickness of this sheet is equal to the chain diameter. The existence of a “sheet”-type configuration is not new for rigid-chain polymers. This class of polymers includes proteins for which the existence of such a configuration is a proven fact [34]. It is called the “cross β-form” or the “β-sheet”.

At the second stage, the sheets unite with one another to form flat aggregates of various sizes with the thickness equal to that of the chain.

The occurrence of flat aggregates makes it possible to explain the experimental results presented in Fig. 3. For this purpose, let us apply the continual model of statistically rough surface [35]. We assume that such a surface, on average, is a plane described by the equation

$$Z = 0. \tag{14}$$

The real surface equation is a random function

$$Z = Z(\mathbf{r}), \tag{15}$$

where $\mathbf{r}$ is a vector with the x- and y-components. Let $R_{\rm c}$ denote the correlation radius for function (15). It is known that, by the order of magnitude, $R_{\rm c}$ is identical to the average inhomogeneity size. We also use $L_{\rm A}$ to denote the size of a flat aggregate.

Assume that the following conditions are satisfied:

$$D \ll R_{\rm c}, \tag{16}$$

$$L_{\rm A} \gg R_{\rm c}. \tag{17}$$

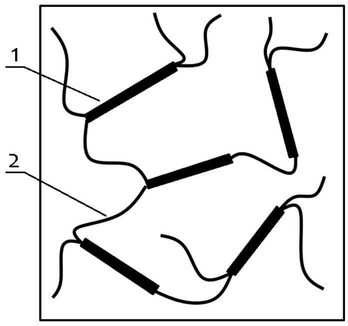

Fig. 4. Model of a network formed by rigid chains: flat aggregates of polymer chains (*1*), chains (*2*)

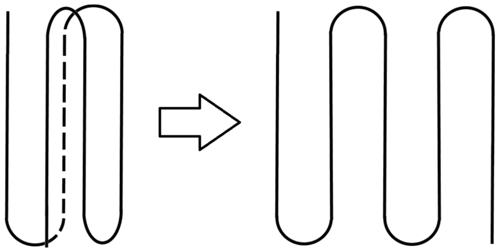

Fig. 5. Unfolding of a globule into a sheet

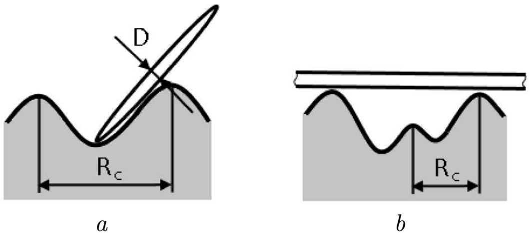

Fig. 6. Contact of globules (*a*) and flat aggregates (*b*) with the substrate surface

Condition (16) means that, at the deposition of an ellipsoidal globule onto the substrate, one of globule’s ends enters a dip on the substrate surface (Fig. 6, *a*), and the long ellipsoid axis turns out inclined with respect to the plane $Z = 0$. The next globules depositing from the solution turn out also inclined to this plane, but at different angles. As a result of this process, a film with substantial surface roughness is formed.

As follows from condition (17), a flat aggregate cannot enter the dip. This is prevented by the humps surrounding the dip. Therefore, the aggregate depositing on the substrate becomes arranged almost in parallel to the plane $Z = 0$ (Fig. 6, *b*). That is why the surface of the formed film turns our to be smoothed, as is evidenced by the experiment.

Note that the presented deposition model is rather approximate, because it does not consider, for example, the translational and rotational Brownian motions of globule-rods [36], as well as their interaction, which undoubtedly affects the roughness of the surface formed during the polymer film epitaxy. The corresponding problem is rather complicated and goes beyond the scope of this work. However, in our opinion, the proposed mechanism of network formation together with the simple deposition model make it possible to qualitatively describe the experimental data obtained using the atomic force microscopy method.

4. Conclusions

On the basis of the research carried out in this work, the following mechanism of network formation in the solutions of rigid-chain polymers can be proposed.

At temperatures below the temperature of the sol-gel transition, the polymer chains have a globule-like configuration: they are elongated ellipsoids of rotation, and the ratios of the lengths of their axes are of an order of several tens. At a temperature exceeding the indicated one, the process of network formation begins. It consists of two stages. At the first stage, the globules unfold. So, the chain acquires a sheet-like configuration. A sheet is formed by a chain that is folded several times. The sheet has a thickness equal to one nanometer by order of magnitude. At the second stage, the sheets unite to form flat aggregates with a thickness of an order of one nanometer. As a result, there arises a network consisting of flat aggregates connected with one another via separate chains.

1. A.R. Khokhlov, A.Yu. Grosberg, V.S. Pande. *Statistical Physics of Macromolecules* (American Institute of Physics, 1994) [ISBN: 978-1563960710].
2. P.-G. Gennes. *Scaling Concepts in Polymer Physics* (Cornell University Press, 1979) [ISBN: 978-0801412035].
3. M. Rubinstein, R.H. Colby. *Polymer Physics* (Oxford University Press, 2003) [ISBN: 978-0198520597].
4. R.A. Siegel, C. Alvarez-Lorenzo. Hydrogels. In: *Drug Delivery: Fundamentals and Application* (CRC Press, 2016) [ISBN: 978-1482217742].
5. J. Li, D.J. Mooney. Designing hydrogels for controlled drug delivery. *Nat. Rev. Mater.* **1**, 16071 (2016).
6. O.M. Alekseev, Yu.F. Zabashta, V.I. Kovalchuk, M.M. Lazarenko, L.A. Bulavin. The structure of polymer clusters in aqueous solutions of hydroxypropylcellulose. *Ukr. J. Phys.* **64**, 238 (2019).
7. O.M. Alekseev, Yu.F. Zabashta, V.I. Kovalchuk, M.M. Lazarenko, E.G. Rudnikov, L.A. Bulavin. Structural transition in dilute solutions of rod-like macromolecules. *Ukr. J. Phys.* **65**, 50 (2020).
8. V.I. Kovalchuk. Phase separation dynamics in aqueous solutions of thermoresponsive polymers. *Cond. Matt. Phys.* **24**, 43601 (2021).
9. Yu.F. Zabashta, V.I. Kovalchuk, L.A. Bulavin. Kinetics of the first-order phase transition in a varying temperature field. *Ukr. J. Phys.* **66**, 978 (2021).
10. V.I. Kovalchuk, O.M. Alekseev, M.M. Lazarenko. Turbidimetric monitoring of phase separation in aqueous solutions of thermoresponsive polymers. *J. Nano- Electron. Phys.* **14**, 01004 (2022).
11. Yu.F. Zabashta, V.I. Kovalchuk, O.S. Svechnikova, L.A. Bulavin. Determination of the surface tension coefficient of polymer gel. *Ukr. J. Phys.* **67**, 365 (2022).
12. Yu.F. Zabashta, V.I. Kovalchuk, O.S. Svechnikova, L.A. Bulavin. Application of the light scattering method to study the hydrogel surface structure. *Ukr. J. Phys.* **67**, 463 (2022).
13. Yu.F. Zabashta, V.I. Kovalchuk, O.S. Svechnikova, L.A. Bulavin. Electrocapillary properties of hydrogels. *Ukr. J. Phys.* **67**, 658 (2022).
14. A.W. Lloyd, R.G. Faragher, S.P. Denyer. Ocular biomaterials and implants. *Biomaterials.* **22**, 769 (2001).
15. B.H. Koffler, M. McDonald, D.S. Nelinson. Improved signs, symptoms, and quality of life associated with dry eye syndrome: Hydroxypropyl cellulose ophthalmic insert patient registry. *Eye Contact Lens* **36**, 170 (2010).
16. J.L. Drury, D.J. Mooney. Hydrogels for tissue engineering: scaffold design variables and applications. *Biomaterials.* **24**, 4337 (2003).
17. J.A. Hunt, R. Chen, T. van Veena, and N. Bryana. Hydrogels for tissue engineering and regenerative medicine. *J. Mater. Chem. B.* **2**, 5319 (2014).
18. J. Siepmann, R. Siegel, M. Rathbone (Eds). *Fundamentals and Applications of Controlled Release Drug Delivery* (Springer, 2012) [ISBN: 978-1461408802].
19. M.L. Weiner, L.A. Kotkoskie. *Excipient Toxicity and Safety* (CRC Press Inc., 2019) [ISBN: 978-0824782108].
20. K.G. Harding, H.L. Morris, G.K. Patel. Science, medicine and the future: Healing chronic wounds. *BMJ* **324**, 160 (2002).
21. V. Jones, J.E. Grey, K.G. Harding. Wound dressings. *BMJ* **332**, 777 (2006).
22. M.E. Aulton. *Aulton's pharmaceutics: the design and manufacture of medicines* (Churchill Livingstone, 2007) [ISBN: 978-0443101083].
23. E. Caló, V.V. Khutoryanskiy. Biomedical applications of hydrogels: A review of patents and commercial products. *Eur. Polym. J.* **65**, 252 (2014).
24. Metolose: Shin-Etsu Chemical Co., Ltd (Japan). http://www.metolose.jp/en/industrial/metolose.html.

25. J. Herder, A. Adolfsson, A. Larsson. Initial studies of water granulation of eight grades of hypromellose (HPMC). *Int. J. Pharm.* **313**, 57 (2006).
26. Metolose: products. https://www.setylose.com/en/products/healthcare/metolose.
27. Gwyddion. http://gwyddion.net/.
28. B. Wunderlich. *Macromolecular Physics. Vol. 1: Crystal Structure, Morphology, Defects* (Academic Press, 1973) [ISBN: 978-0127656014].
29. B.J. Berne, R. Pecora. *Dynamic Light Scattering: With Applications to Chemistry, Biology, and Physics* (Dover Publications, 2000) [ISBN: 978-0486411552].
30. J. Frenkel. *Kinetic Theory of Liquids* (Dover Publications, 1955) [ASIN: B000ELFWHG].
31. F. Perrin. Mouvement Brownien d'un ellipsoide (I). Dispersion dièlectrique pour des molècules ellipsoidales. *J. Phys. Radium* **5** (10), 497 (1934).
32. F. Perrin. Mouvement Brownien d'un ellipsoide (II). Rotation libre et dèpolarisation des fluorescences. Translation et diffusion de molècules ellipsoidales. *J. Phys. Radium* **7**, 1 (1936).
33. H. Yamakawa. *Modern Theory of Polymer Solutions* (Harper & Row, 1971) [ISBN: 978-0060473099].
34. J.D. Watson, F.H. Crick. Molecular structure of nucleic acids: A structure for deoxyribose nucleic acid. *Nature* **171**, 737 (1953).
35. F.G. Bass, I.M. Fuks. *Wave Scattering from Statistically Rough Surfaces* (Pergamon, 1979) [ISBN: 978-1483187754].
36. N.I. Lebovka, Yu.Yu. Tarasevich, L.A. Bulavin, V.I. Kovalchuk, N.V. Vygornitskii. Sedimentation of a suspension of rods: Monte Carlo simulation of a continuous two-dimensional problem. *Phys. Rev. E* **99**, 052135 (2019).

Received 05.03.23.
Translated from Ukrainian by O.I. Voitenko

Ю.Ф. Забашта, В.І. Ковальчук,
О.С. Свечнікова, С.В. Кондратенко, С.О. Алексеев,
А.В. Британ, Л.Ю. Вергун, Л.А. Булавін

ОСОБЛИВОСТІ УТВОРЕННЯ СІТКИ В ГЕЛЯХ ЖОРСТКОЛАНЦЮГОВИХ ПОЛІМЕРІВ

Показано, що сітка в гелях жорстколанцюгових полімерів має специфічну форму – в цій сітці роль вузлів відіграють плоскі агрегати, утворені складеними полімерними ланцюгами. Пропонується механізм виникнення такої сітки. Її існування для гідрогелів метолози підтверджено експериментально за допомогою методів динамічного розсіяння світла та атомно-силової мікроскопії.

Ключові слова: полімерна сітка, динамічне розсіяння світла, атомно-силова мікроскопія.